Available online at www.sciencedirect.com
ScienceDirect
Catalysis Today 131 (2008) 90–97
CATALYSIS TODAY
www.elsevier.com/locate/cattod

Analytical TEM observation of Au–Pd nanoparticles prepared by sonochemical method

T. Akita [a,*], T. Hiroki [b], S. Tanaka [a], T. Kojima [c], M. Kohyama [a], A. Iwase [b], F. Hori [b]

[a] *Research Institute for Ubiquitous Energy Devices, National Institute of Advanced Industrial Science and Technology (AIST), Midorigaoka1-8-31, Ikeda, Osaka 563-8577, Japan*
[b] *Department of Materials Science, Osaka Prefecture University, Gakuen-cho1-1, Sakai, Osaka 599-8531, Japan*
[c] *Radiation Research Center, Osaka Prefecture University, Gakuen-cho 1-2, Sakai, Osaka 599-8570, Japan*

Available online 3 December 2007

Abstract

The Au–Pd nanoparticles prepared by sonochemical technique were investigated by the analytical transmission electron microscopy. The core (Au)–shell (Pd) structure without apparent mixing layers and with similar thickness of Pd shells was clearly confirmed by the image and intensity profile of annular dark field scanning transmission electron microscopy (ADF-STEM) and also by the line-scan analysis of energy dispersive X-ray spectroscopy (EDS) in STEM mode. Detailed analyses of the ADF-STEM imaging, the electron diffraction pattern and the FFT pattern of HRTEM images complementarily show that the Pd shell epitaxially grows on the Au core expanded with the same lattice constant as Au and with the coherent Pd/Au interface structure.

Keywords: TEM; ADF-STEM; EDS; Au–Pd; Nanoparticles; Core–shell

1. Introduction

Noble metal nanoparticles are widely used as catalysts, and bimetallic nanoparticles are also used for various catalytic reactions as represented by Pt–Ru electrocatalysts of proton-exchange membrane fuel cells. Recently, it is reported that the Au–Pd bimetallic particles exhibit high catalytic activity for various reactions. For example, Au–Pd particles supported on metal oxides exhibit high activity for the synthesis of hydrogen peroxide from H_2 and O_2 or the oxidation of alcohols to aldehydes with O_2 [1–3]. Structure analyses by an analytical TEM revealed that the bimetallic Au–Pd particles have a Pd-rich surface [3]. The surface of a Au–Pd alloy was also carefully investigated by surface science techniques, and it was revealed that the isolated Pd atoms surrounded by Au atoms are active for the reaction of acetoxylation of ethylene to vinyl acetate [4].

Thus it is of great importance to understand and control the structures of bimetal particles and the interface between bimetal particles and supports in nano-scale in order to develop new catalysts with excellent performance. Previously the Au–Pd bimetallic nanoparticles were prepared by simultaneous reduction of $HAuCl_4$ and $PdCl_2$, and the extended X-ray absorption fine structure (EXAFS) analyses successfully revealed that the Au–Pd bimetallic nanoparticles had the core–shell structure [5]. Recently, the sonochemical technique is also applied to prepare the Au–Pd or Au–Pt bimetallic nanoparticles more efficiently [6–10]. And the Au–Pd core–shell particles exhibited higher catalytic activity for hydrogenation of 4-pentenoic acid in comparison to Au particles or Pd particles alone. The Au–Pd particles prepared by the sonochemical technique also reveal high catalytic activity for the hydrogenation of cyclohexene when supported on Fe_2O_3 [11]. The structure of the bimetallic particles depends on the preparation conditions. The detailed structure of the bimetallic nanoparticles is not yet understood well, because atomic-scale characterization is difficult for the inside of nanoparticles. It is essential to elucidate the detailed structure of bimetallic Au–Pd nanoparticles in order to understand the catalytic properties. In this study, the structure of Au–Pd nanoparticles prepared by the sonochemical technique is directly investigated by an analytical transmission electron microscopy with annular dark field scanning transmission electron microscopy (ADF-STEM) method.

* Corresponding author. Tel.: +81 72 751 9732; fax: +81 72 751 9714.
E-mail address: t-akita@aist.go.jp (T. Akita).

0920-5861/$ – see front matter © 2007 Elsevier B.V. All rights reserved.
doi:10.1016/j.cattod.2007.10.033

2. Experimental

Bimetallic Au–Pd particles were prepared by the sonochemical techniques [6,7]. A multiwave ultarasonic generator with a barium titanate oscillator of 64 mm diameter was operated for sonication at 200 kHz with an input power of 200 W. The solutions of 0.5 mmol/l $NaAuCl_4{\cdot}2H_2O$ and 0.5 mmol/l $PdCl_2{\cdot}2NaCl{\cdot}3H_2O$ were used as precursors of Au^{3+} and Pd^{2+} ions, respectively. The 60 ml aqueous solutions containing Au and Pd ions with an additive of sodium dodecyl sulfate (SDS) were sonicated in a water bath for 20 min at approximately 293 K [8]. The UV–vis spectra were measured by a spectrometer Shimazu UV-3100.

The structure of the Au–Pd particles was observed by the analytical transmission electron microscope (TEM), JEOL JEM-3000F, equipped with energy dispersive X-ray spectroscopy (EDS), and ADF-STEM systems. The Au–Pd nanoparticles are dispersed on a carbon film supported on Cu-mesh of 3 mm in diameter by dropping the solution including the Au–Pd particles. The unnecessary solution is absorbed by filter paper, and the sample is dried in vacuum. The EDS analyses are carried out by using Thermo Noran VANTAGE EDS analysis system. The specimen drift-correction programs are used for the EDS line-scan analyses. The fast fourier-transform (FFT) analyses of TEM images are carried out by image analysis software, Gatan Digital Micrograph. The ADF-STEM images are obtained with a collection angle of 65 to 255 mrad with 0.2–0.3 nm electron probe.

3. Results and discussion

Fig. 1 shows UV–vis spectra during the synthesis of Au–Pd bimetallic nanoparticles. Each spectrum was obtained from the abstracted samples at each reaction time. An absorption peak (plasmon peak) due to Au particles located around 520 nm [8] appears clearly at about 6 min after the start of sonication. An absorption peak around 300 nm is due to the $AuCl^{4-}$ complex, and it is only observed at the early stage of sonication. The absorption peak at 520 nm gradually disappears after 9 min, which indicates the Pd-layer coverage over Au particles. These experimental results indicate that the reduction of Au^{3+} occurs initially, followed by the Pd^{2+} ion reduction so as to cover the Au particles, which indirectly shows the formation of the Au-core and Pd-shell structure [8].

A typical TEM image of prepared Au–Pd nanoparticles with size distribution is presented in Fig. 2. Bimetallic Au–Pd nanoparticles with an averaged diameter of 13 ± 3.2 nm are successfully prepared by the sonochemical method. Some particles show single crystalline structure in HRTEM images, but many particles include defect structure such as multiple twins which are often observed in noble metal particles [12]. The bimetallic Au–Pd nanoparticles also have polyhedral shapes with low index facets such as {1 1 1} or {1 0 0}. EDS analyses confirmed that each nanoparticle is really composed of Au and Pd. Residual Na or Cl from precursors of Au and Pd ions is sometimes observed as small crystals of NaCl, but the amount of Na and Cl contained in the Au–Pd nanoparticles is below the detection limit of EDS analysis. The Au–Pd nanoparticles are stable under electron beam irradiation of

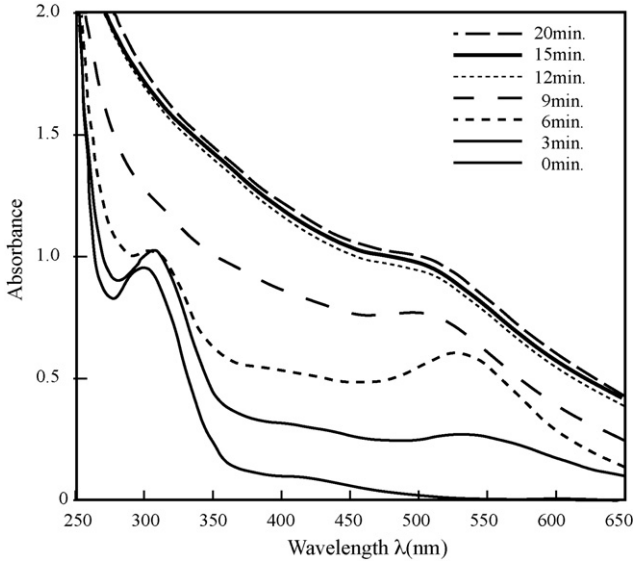

Fig. 1. UV–vis spectra during the synthesis of Au–Pd bimetallic nanoparticles by sonochemical technique.

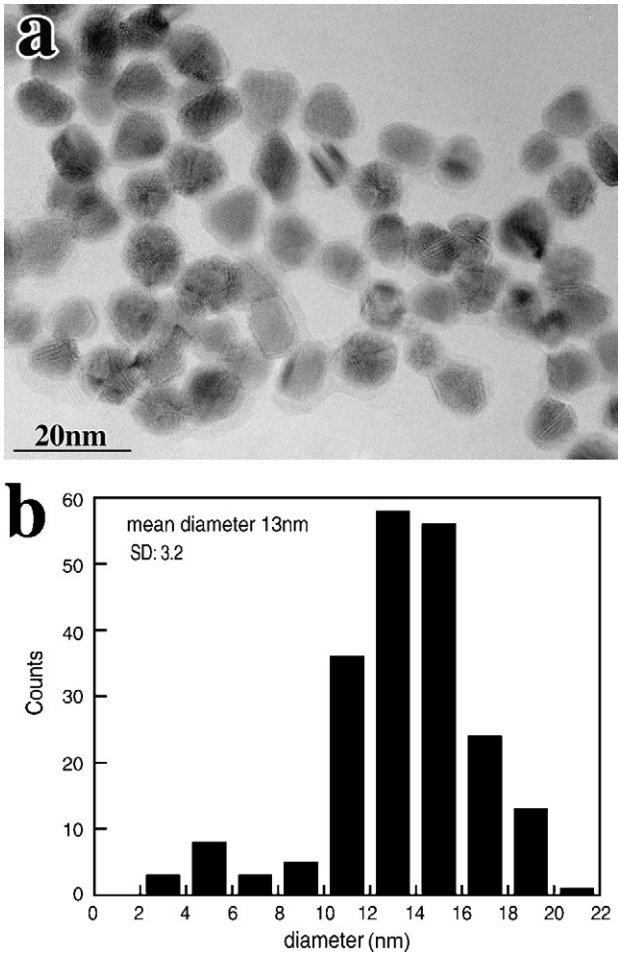

Fig. 2. A typical TEM image of Au–Pd nanoparticles prepared by sonochemical method (a) and size distribution of the Au–Pd particles (b).

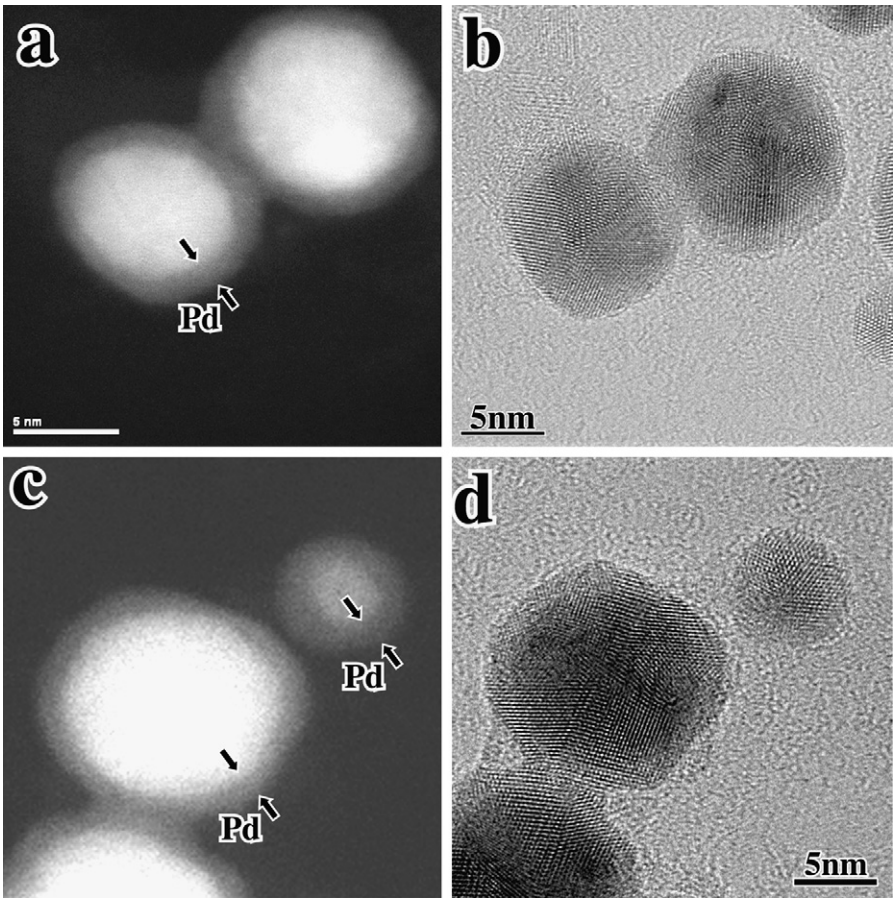

Fig. 3. ADF-STEM (a, c) and TEM (b, d) images of Au–Pd nanoparticles.

300 kV during conventional HRTEM observation with current density of about 1×10^5 A/m^2. No obvious structure changes of the particles are observed during TEM observation and EDS measurements.

It is difficult to confirm the core–shell structure directly through the diffraction and phase contrasts of a conventional TEM, although the ADF-STEM observation [13,14] is effective to examine the core–shell structure. ADF-STEM images are shown in Fig. 3a and c obtained from the same areas in TEM images in Fig. 3b and d, respectively. In the TEM images, the lattice fringes are observed for various directions in Au–Pd nanoparticles, which means that particles are not necessarily single crystals but include stacking faults. In the ADF-STEM images, the particles reveal bright contrast, where strongly bright region is surrounded by weaker contrast region as indicated by arrows. The image intensity of an ADF-STEM image is almost proportional to the square of the *Z*-number of elements in the sample when the sufficient collection angle is used [15]. Thus the core (Au)–shell (Pd) structure can be identified by the difference of the *Z*-number between Au (79) and Pd (46). The mean thickness of a Pd shell is estimated to be about 1.3 nm from the ADF-STEM images. For the small Au–Pd nanoparticle of about 5 nm in diameter at the upper right side in Fig. 3c and d, the shell thickness is almost the same as that of larger particles. It is noteworthy that the thickness of a Pd layer is almost the same, independent of the size of an Au core. This should be because the Pd shell grows uniformly on the surface of each Au particle after the reduction of Au. Although the composition ratio of Au and Pd for the small particles will be deviated from the mean composition (1:1), the deviation will be compensated by the fluctuation of many Au–Pd particles which have diameters of near mean value because the number of the Au–Pd particles about 5 nm in diameter is small.

The intensity profile of the ADF-STEM image is shown in Fig. 4. The profile along the line in Fig. 4a is plotted by a solid line in Fig. 4b. An expected intensity profile is also plotted by solid squares in Fig. 4b, which is simulated by supposing that the image intensity of the ADF-STEM is simply proportional to the square of *Z*-number and the thickness along the projected direction for each Au-core and Pd-shell regions with ideal spherical shapes and ideal atomic densities [13]. The spreading of spatial resolution by the probe size is not considered. The observed profile is well fitted by the expected profile simulated for the particle with an Au core of 8 nm diameter and a Pd shell of 1 nm thickness. The deviation is due to the incomplete spherical shape of the real particle and the probe-size effect. It seems that Au and Pd are almost separated without forming an apparent alloy phase, although it is unknown whether the intermixing layers exist or not at the interface region within a few atomic layers.

The line-scan EDS analysis was also carried out in STEM mode in order to confirm the local composition of the core

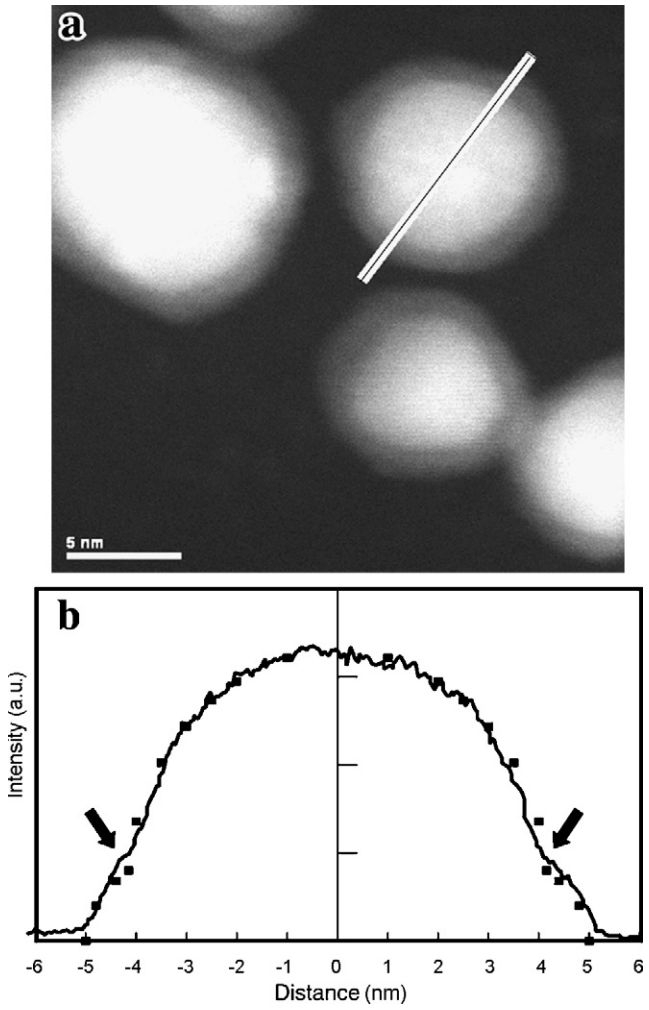

Fig. 4. ADF-STEM image of Au–Pd nanoparticles (a) and intensity profile of the ADF-STEM image of one Au–Pd nanoparticle (b). The calculated profile is indicated by solid squares.

(Au)–shell (Pd) structure. The intensity profile of Au-Mα and Pd-Lα X-rays is plotted in Fig. 5b along the line on the Au–Pd nanoparticle of the ADF-STEM image in Fig. 5a. Ten points were measured in every 4 s along the line, and the X ray signals for each point were accumulated 20 times repeatedly. The spatial drift of the sample was corrected every 10 s using a sample drift-correction program based on the calculation of the image correlation. In order to estimate the background intensity of X-rays, the X-ray intensity corresponding to the Fe–K line, of which the element is absent in the sample, is also plotted. The EDS intensity profile also indicates that the Pd shell really exists around the Au core. The ideal EDS intensity profile supposing the ideal spherical and separated core–shell structure is also plotted by broken lines in Fig. 5b. There are substantial differences between the observed and ideal profiles, which should be mainly caused by the specimen drift within 10 s of the drift-correction process as well as the practical spatial resolution of the EDS line analysis of about 1 nm.

In order to investigate the crystal structure of the Au core and Pd shell, selected area (SA) electron diffraction pattern was obtained from the Au–Pd nanoparticles as shown in Fig. 6. The intensity profile of the diffraction pattern obtained from the rotational average is plotted in Fig. 6b. The same kind of profile from Au particles supported on an amorphous carbon film is also plotted for comparison. The SA electron diffraction pattern shows Debye ring pattern. There are no diffraction rings corresponding to the lattice constant of bulk fcc Pd in the diffraction pattern of the Au–Pd particles. In contrast, the diffraction rings corresponding to the lattice constant of bulk Au are just observed in the diffraction pattern of the Au–Pd particles. The difference in the lattice constants between Au ($a = 0.4079$ nm) and Pd ($a = 0.3890$ nm) is about 5% and enough to detect in the resolution of the present electron diffraction experiment. In the intensity profile for the Au–Pd

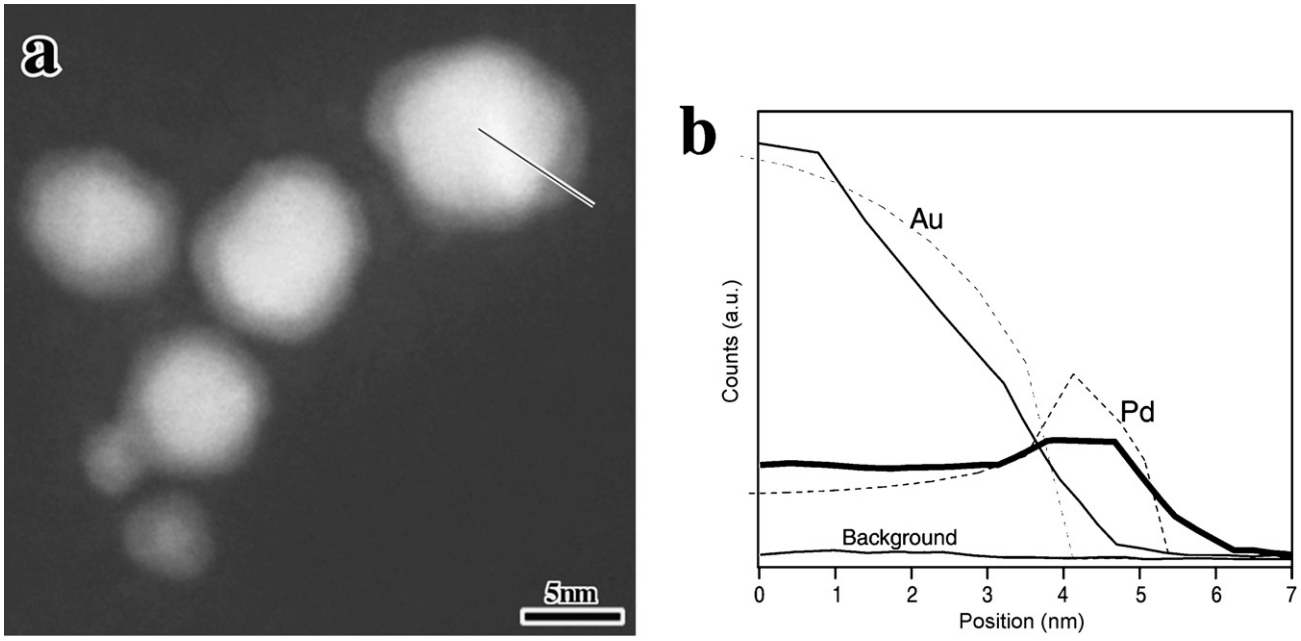

Fig. 5. ADF-STEM image (a) and EDS intensity profile of the Au–Pd nanoparticle (b). The EDS intensity profile is obtained along the line. The calculated EDS intensity profile is indicated by broken lines.

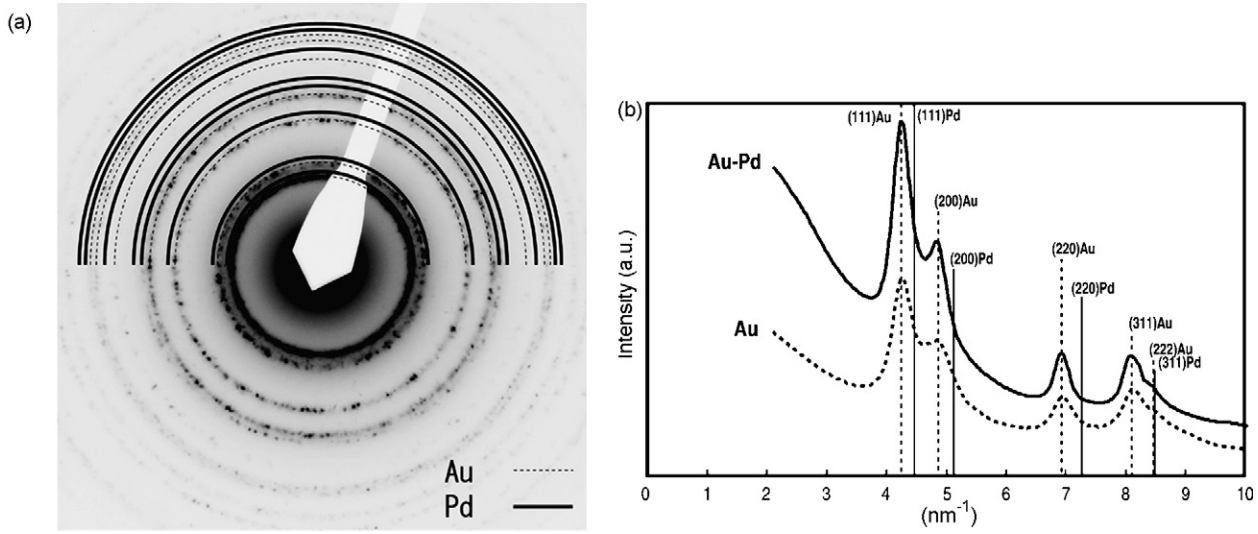

Fig. 6. Selected area electron diffraction pattern of Au–Pd nanoparticles (a) and intensity profile of the electron diffraction pattern of Au–Pd nanoparticles and Au particles (b). Ideal peak positions of bulk Pd and bulk Au are indicated by solid and broken vertical lines, respectively.

particles in Fig. 6b, the peak positions are the same as those of the Au particles. The measurement error in the intensity profile mainly comes from the accuracy in the definition of the center of diffraction pattern during the rotational average process. No diffraction peaks of bulk Pd indicate the possibility that the lattice constant of Pd is changed and coincides with that of Au through some kind of pseudomorphic growth of Pd on an Au core. Another possible reason is that the diffraction intensity

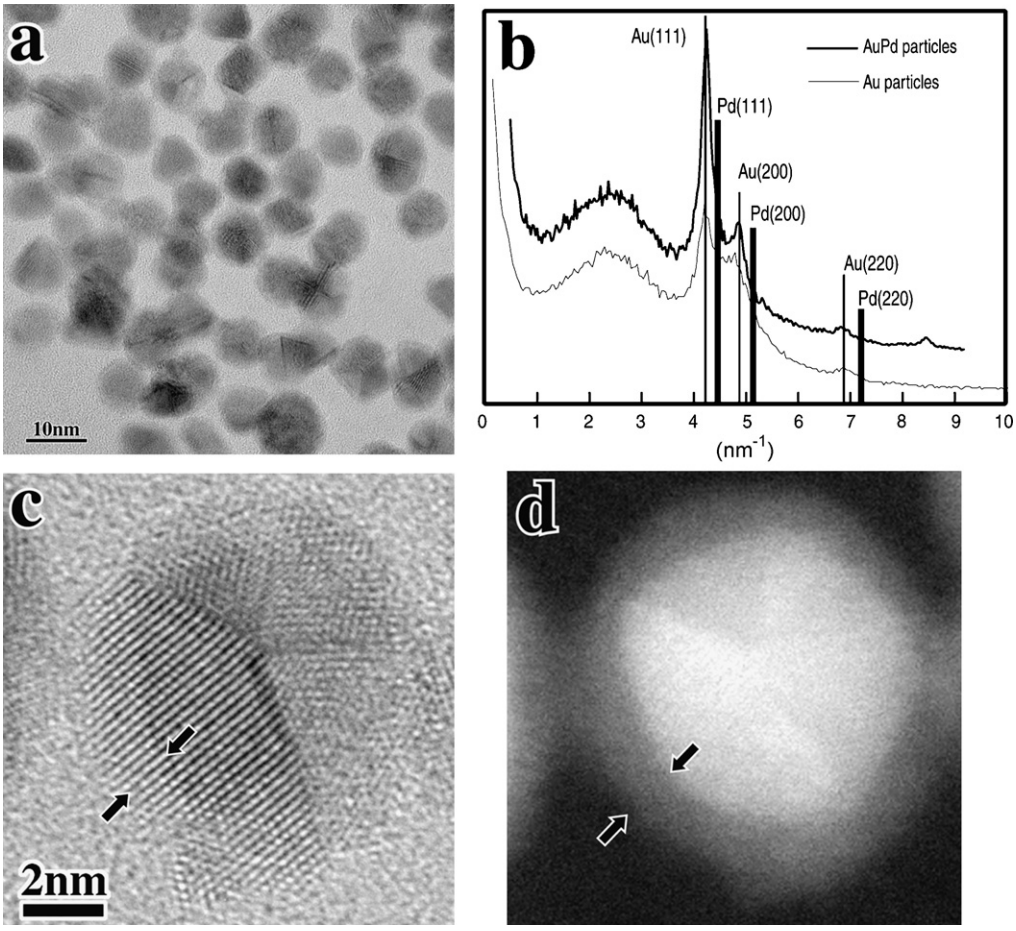

Fig. 7. HRTEM (a, c) and ADF-STEM (d) images of Au–Pd nanoparticles, and intensity profile of FFT pattern (b) obtained from the HRTEM image (a). Ideal peak positions of bulk Pd and bulk Au are indicated by thick and thin vertical lines, respectively, in (b).

from a Pd shell is not enough due to the thickness of 1 nm. Previous X-ray diffraction analyses for Au–Pd nanoparticles also indicated that there were no diffraction peaks corresponding to the bulk Pd [7].

The lattice spacing in the Au–Pd nanoparticles observed in HRTEM images was also analyzed by the FFT pattern. Fig. 7b shows the radial averaged profile of the FFT pattern obtained from the digitally processed HRTEM image of 4096 × 4096 pixels in Fig. 7a. One pixel corresponds to 0.018 nm, and various lattice fringes are clearly observed in the HRTEM image with enough spatial resolution. The FFT profile of the TEM image of the Au particles deposited on carbon micro-grid

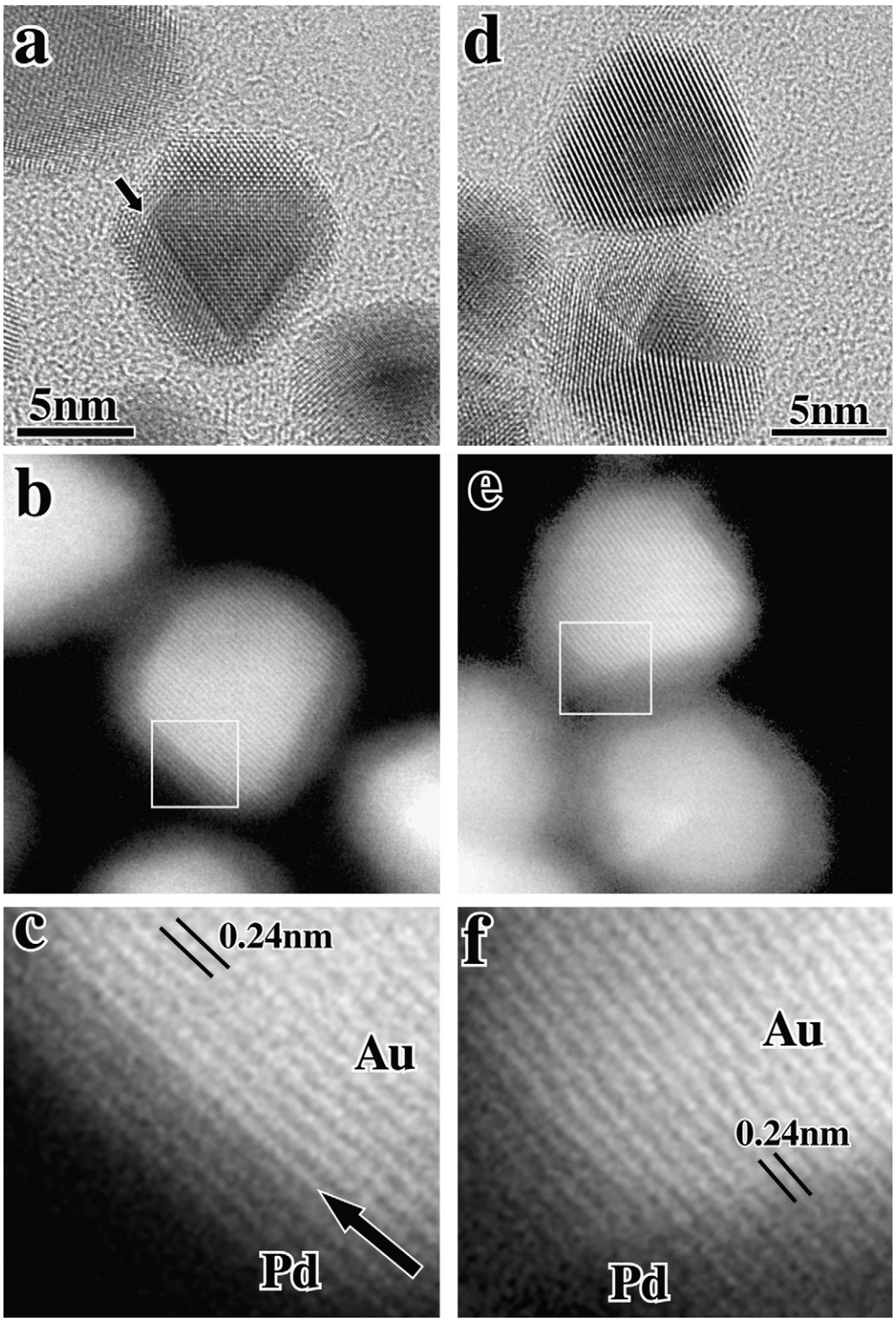

Fig. 8. HRTEM image of Au–Pd nanoparticles (a, d) and corresponding ADF-STEM images of Au–Pd nanoparticles (b, e). The enlarged ADF-STEM images (c, f) from the white rectangle in the ADF-STEM images (b) and (e).

is also shown in Fig. 7b for comparison. In Fig. 7c, the lattice fringes are observed in the edge of the Au–Pd particle. This region is considered as a Pd-shell region indicated by the same arrows in the ADF-STEM image of Fig. 7d. Thus the FFT pattern from the HRTEM images indeed contains the components of lattice fringes of Pd crystal regions. However, there are again no peaks corresponding to the lattice constant of bulk Pd in the FFT pattern profile in Fig. 7b. Only Au peaks corresponding to the low index lattice planes such as Au(1 1 1), Au(2 0 0), and Au(2 2 0) are observed, and no peak shifts caused by the Au–Pd alloy formation are seen. Thus it is feasible that the lattice constant of the Pd crystal is expanded to be similar to the Au lattice through epitaxial growth of Pd on the Au core. There is an experimental report on the pseudomorphic growth of a Pd film on a single crystalline Au(1 0 0) substrate with the same lattice constant as the Au lattice within 6–9 layers [16]. Thus it is probable that the Pd shell reveals the lattice constant similar to the Au core, because the Pd shell has a thickness of 4–5 atomic layers in the present samples.

Further HRTEM and ADF-STEM observations were carried out so as to clarify the Au/Pd interface structure in atomic scale. Fig. 8 shows HRTEM and ADF-STEM images for the same particles. Fig. 8c and f shows enlarged ADF-STEM images of the Pd/Au interfaces indicated in Fig. 8b and e. The ADF-STEM observations were successful in identifying the Pd/Au interface with enough image contrast. In the HRTEM image in Fig. 8a, the position of the Pd/Au interface is not clear, because the diffraction contrast by stacking faults disturbs the identification of the interface as indicated by an arrow. In contrast, the ADF-STEM images in Fig. 8b and 8c clearly show the interface position. In Fig. 8c, we can see that 4–5 layers of Pd are formed on the Au particle with the epitaxial relationship of (1 1 1)Au//(1 1 1)Pd. The coherent epitaxy is also obvious in Fig. 8e and f. In Fig. 8f, the phase shift of lattice fringe between the Au core and the Pd shell is not seen at the interface. All the interfaces seem to be abrupt, while it is unknown in the ADF-STEM images whether the intermixing layer of Au and Pd exists or not at the interface. In this experiment, the sensitivity is not enough to distinguish the kind of atoms quantitatively in atomic scale. It was reported by Kan et al. that poly-crystalline Pd shells covered Au cores without epitaxial relationship [10]. This difference seems to be caused by the differences in precursors or additives used for the synthesis of Au–Pd nanoparticles.

The lattice space in the Pd layer is not estimated directly from these ADF-STEM images because the image contrast and spatial resolution are not enough for the precise estimation with accuracy of a few percent. However, all the present results of the electron diffraction, the FFT analysis of HRTEM images and the ADF-STEM observations complementarily indicate that Pd layers pseudomorphically grow on Au cores with the same lattice constant as Au and with the coherent interface structure. This is one of the possible reasons for the higher catalytic activity of the Au–Pd nanoparticles than that of Au or Pd particles. It is interesting to investigate how the change of the lattice constant of Pd affects the catalytic properties.

Finally, it is of quite interest to examine the effects of increasing the thickness of the Pd shell on the crystal structure of Pd or on the interface structure in the near future. This should provide insight into the mechanism of the present coherent growth of Pd. And also it is important to examine the thermal stability of the Au–Pd core–shell structure in the future. There is a possibility that the present core–shell structure is non-equilibrium state or stabilized by residual impurities contained during synthesis. In the present study, the Au–Pd core–shell particles were stable at least during the TEM observations. The surface segregation of Au atoms in the Au–Pd alloy surface was observed during annealing process as theoretically predicted [17,18]. Thus the Au atoms may segregate on the surface of the bimetallic particle in the equilibrium state.

4. Conclusion

Detailed structure of bimetallic Au–Pd nanoparticles prepared by the sonochemical technique was examined by an analytical TEM. The following conclusions have been drawn:

(1) The Au-core Pd-shell structure without apparent alloy regions and with similar thickness of Pd shells was clearly confirmed by ADF-STEM and EDS line analyses.
(2) The coherent Pd/Au interface via the epitaxial growth of Pd shells was observed by HRTEM and ADF-STEM.
(3) The results of HRTEM, ADF-STEM and electron diffraction analyses complementarily indicate that the Pd lattice is expanded and coincides with the Au lattice.

Acknowledgements

This work was supported by the Japan Society for the Promotion of Science (JSPS-Grant-in-Aid for Scientific Research (B) 17360314). The authors are grateful to Drs. S. Ichikawa (Osaka University), K. Okazaki (JST), and K. Tanaka (AIST) for their valuable comments and stimulating discussions.

References

[1] J.K. Edwards, B. Solsona, P. Landon, A.F. Carley, A. Herzing, M. Watanabe, C.J. Kielyb, G.J. Hutchings, J. Mater. Chem. 15 (2005) 4595.
[2] D.I. Enache, J.K. Edwards, P. Landon, B. Solsona-Espriu, A.F. Carley, A.A. Herzing, M. Watanabe, C.J. Kiely, D.W. Knight, G.J. Hutchings, Science 311 (2006) 362.
[3] B.E. Solsona, J.K. Edwards, P. Landon, A.F. Carley, A. Herzing, C.J. Kiely, G.J. Hutchings, Chem. Mater. 18 (2006) 2689.
[4] M. Chen, D. Kumar, C.-W. Yi, D.W. Goodman, Science 310 (2005) 291.
[5] N. Toshima, M. Harada, Y. Yamazaki, K. Asakura, J. Phys. Chem. 96 (1992) 9927.
[6] Y. Mizukoshi, K. Okitsu, Y. Maeda, T.A. Yamamoto, R. Oshima, T. Nagata, J. Phys. Chem. B 101 (1997) 7033.
[7] Y. Mizukoshi, T. Fujimoto, Y. Nagata, R. Oshima, Y. Maeda, J. Phys. Chem. B 104 (2000) 6028.
[8] H. Takatani, H. Kago, Y. Kobayashi, F. Hori, R. Oshima, Trans. Mater. Res. Soc. Jpn. 28 (2003) 871.
[9] M. Nakanishi, H. Takatani, Y. Kobayashi, F. Hori, R. Taniguchi, A. Iwase, R. Oshima, Appl. Surf. Sci. 241 (2005) 209.

[10] C. Kan, W. Cai, C. Li, L. Zhang, H. Hofmeister, J. Phys. D: Appl. Phys. 36 (2003) 1609.
[11] H. Nitani, M. Yuya, T. Ono, T. Nakagawa, S. Seino, K. Okitsu, Y. Mizukoshi, S. Emura, T.A. Yamamoto, J. Nanoparticle Res. 8 (2006) 951.
[12] S. Ino, J. Phys. Soc. Jpn. 21 (1966) 346.
[13] Z.Y. Li, J. Yuan, Y. Chen, R.E. Palmer, J.P. Wilcoxon, Appl. Phys. Lett. 87 (2005) 243103.
[14] J.-W. Hu, Y. Zhang, J.-F. Li, Z. Liu, B. Ren, S.-G. Sun, Z.-Q. Tian, T. Lian, Chem. Phys. Lett. 408 (2005) 354.
[15] S.J. Pennycook, Ultramicroscopy 30 (1989) 58.
[16] A.L.N. Pinheiro, M.S. Zei, M.F. Luo, G. Ertl, Surf. Sci. 600 (2006) 641.
[17] C.-W. Yi, K. Luo, T. Wei, D.W. Goodman, J. Phys. Chem. B109 (2005) 18535.
[18] A.V. Ruban, H.L. Skriver, J.K. Nørskov, Phys. Rev. B59 (1999) 15990.